

A New Route to Obtain High-Yield Multiple-Shaped Gold Nanoparticles in Aqueous Solution using Microwave Irradiation

Subrata Kundu,* Luohan Peng, and Hong Liang*

Materials Science and Mechanical Engineering, Texas A & M University, College Station, Texas 77843-3123

Received March 6, 2008

A highly effective, very fast microwave method is described to synthesize shape controlled gold nanoparticles in the presence of 2,7-dihydroxy naphthalene (2,7-DHN) as a new reducing agent under microwave heating for 60–90 s. The growth of the particles with different shapes (spherical, polygonal, rod, and triangular/prisms) was directed by the surfactant to metal ion molar ratios and the concentration of 2,7-DHN. The evolved nanorods and nanoprisms are fairly small in diameter, and the particle size and shape were successfully tuned just by varying the molar ratios of the reactants. The process presented here can be extended to the synthesis of other nanomaterials with desired size and shape and might find a variety of applications in wide areas, such as catalysis, clinical and diagnostic medicine, and nanoelectronics.

Introduction

In the past few years, nanomaterials research has attracted enormous attention because of the variety of unique spectroscopic,¹ electronic,² and chemical³ properties that arises from the nanoparticles (NPs) small size and large surface to volume ratio. These NPs have found wide applications in the fields of physics,⁴ chemistry,⁵ biology,⁶ medicine,⁷ materials science,⁸ and other interdisciplinary fields in engineering. Among a wide variety of NPs studied, gold is of particular interest because of its fascinating properties and potential applications in catalysis,⁹ drug delivery,¹⁰ optoelectronics,¹¹ and magnetic devices.¹² There are many

processes developed for the synthesis of gold NPs.^{13–16} Among those, the chemical reduction remains the most popular. As NPs tend to be unstable in a solution, special precautions have to be taken to avoid their agglomeration and/or precipitation.

There are reports on the development of simple ways to synthesize size- and shape-controlled nanomaterials, such as nanocubes, nanorods, nanowires, nanodisks, nanotapes, nanobelts, nanotetrapods, among others.^{13–15} Methods include chemical, physical, biological, and photoreduction.^{13–16} Shape controlled gold NPs have been synthesized in the presence of different beta-diketones as chelating ligands.¹⁷ However, all these above-mentioned methods were found to be time-consuming, and particles were found in general to be large with uncontrollable size distribution. The microwave chemistry has recently been reported to be effective in making size and shape controlled metallic NPs. The microwave irradiation (MWI) has a rapid heating capacity with a high penetration power. The importance of the microwave heating lies in the fact that it can heat a substance uniformly and generate homogeneous nucleation

* To whom correspondence should be addressed. E-mail: skundu@tam.u.edu (S.K), hliang@tam.u.edu (H.L). Phone: 979-862-2578. Fax: 979-845-3081.

- (1) Henglein, A. *J. Phys. Chem.* **1993**, *97*, 5457.
- (2) Kundu, S.; Liang, H. *Adv. Mater.* **2008**, *20*, 826.
- (3) El-Sayed, M. A. *Acc. Chem. Res.* **2001**, *34*, 257.
- (4) Bae, S.; Lee, S. W.; Takemura, Y. *Appl. Phys. Lett.* **2006**, *89*, 252506.
- (5) Daniel, M.; Astruc, D. *Chem. Rev.* **2004**, *104*, 293.
- (6) Bauer, L. A.; Birenbaum, N. S.; Mayer, G. *J. Mater. Chem.* **2004**, *14*, 517.
- (7) Haes, A. J.; Van Duyne, R. P. *J. Am. Chem. Soc.* **2002**, *124*, 10596.
- (8) Niemeyer, C. M.; Doz, P. *Angew. Chem., Int. Ed.* **2001**, *40*, 4128.
- (9) Crooks, R. M.; Zhao, M.; Sun, L.; Chechik, V.; Yeung, L. K. *Acc. Chem. Res.* **2001**, *34*, 181.
- (10) Neuberger, T.; Bchöpf, S.; Hofmann, H.; Hofmann, M.; Rechenberg, B. *J. Magn. Magn. Mater.* **2005**, *293*, 483.
- (11) Taleb, A.; Petit, C.; Pileni, M. P. *J. Phys. Chem. B* **1998**, *102*, 2214.
- (12) Sun, S.; Murray, C. B.; Weller, D.; Folks, L.; Moser, A. *Science* **2000**, *287*, 1989.

- (13) Murphy, C. J.; Jana, N. R. *Adv. Mater.* **2002**, *14*, 80.
- (14) Sun, Y.; Mayers, B.; Xia, Y. *Adv. Mater.* **2003**, *15*, 641.
- (15) Kundu, S.; Panigrahi, S.; Praharaj, S.; Basu, S.; Ghosh, S. K.; Pal, A.; Pal, T. *Nanotechnology* **2007**, *18*, 75712.
- (16) Pol, V. G.; Srivastava, D. N.; Palchik, V.; Slifkin, M. A.; Weiss, A. M.; Gedanken, A. *Langmuir* **2002**, *18*, 3352.
- (17) Kundu, S.; Pal, A.; Ghosh, S. K.; Nath, S.; Panigrahi, S.; Praharaj, S.; Pal, T. *Inorg. Chem.* **2004**, *43*, 5489.

sites as compared to those of conventional heating. The MW heating method has been used to synthesize spherical NPs of metals like Au,¹⁸ Ag,¹⁹ Pd,¹⁸ Pt,²⁰ and so forth and semiconductor nanorods and wires²¹ at a high speed. There is no report for the controlled synthesis of nanorods and nanoprisms using the MW heating method. Murphy et al. synthesized gold nanorods using a seed mediated approach.¹³ Mirkin et al.²² synthesized silver nanoprisms by irradiating with UV-light for 70 h. Shastry et al.²³ synthesized large size (0.05–1.8 μm) gold nanoprisms by extracting a lemongrass plant through conventional heating methods. Recently, Chung et al.²⁴ synthesized 98 ± 17 nm gold nanoprisms by seed mediated methods. Using this method, the yields of nanoprisms was very low, $\sim 45 \pm 5\%$. As seen, all the above-mentioned methods for making shape controlled NPs require multiple steps, high temperature, long time, or results in mixed particles of different shapes with lower yields.

In this present research, we developed a process using a microwave to synthesize shape controlled (spherical, polygonal, rods, and prisms) gold NPs in a reaction time of less than 90 s in the presence of a cationic surfactant. The reduction of gold salt was done in CTAB (cetyl trimethyl ammonium bromide) micellar media in the presence of alkaline 2,7-dihydroxy naphthalene (2,7-DHN) as a new reducing agent. This method generates exclusively spherical, polygonal, rods, and triangular gold NPs within a short time. The particle size and shape can be tuned just by varying the metal salt to surfactant molar ratio and by changing the concentration of 2,7-DHN and the MW heating time. To our best knowledge, shape controlled gold NPs synthesized within 90 s have not been reported. The yield of the NPs like nanorods (aspect ratio ~ 12) and nanoprisms (size ~ 65 nm) is very high ($>85\%$), and the present approach is straightforward, simple, cost-effective, and less time-consuming.

Experimental Details

Reagents. 2,7-Dihydroxy naphthalene (2,7-DHN), 2-naphthol (2-N), and 1,2-dihydroxy naphthalene (1,2-DHN) were purchased from Sigma-Aldrich and were recrystallized in hot water. Cetyltrimethyl ammonium bromide (CTAB, 99%), sodium lauryl sulfate (SDS), and hydrogen tetrachloro aurate, trihydrate ($\text{HAuCl}_4 \cdot 3\text{H}_2\text{O}$, 99.9%) were purchased all from Sigma-Aldrich and were used without further purification. Other chemicals like polyallylamine hydrochloride (PAH, Polymer Scientific Products, Ltd.) and sodium hydroxide (NaOH, Sigma-Aldrich) were used as received. Ultra pure distilled (UPD) water was used for the entire synthesis.

Instruments. UV–visible absorption spectra were recorded in the Hitachi (model U-4100) UV–vis–NIR spectrophotometer

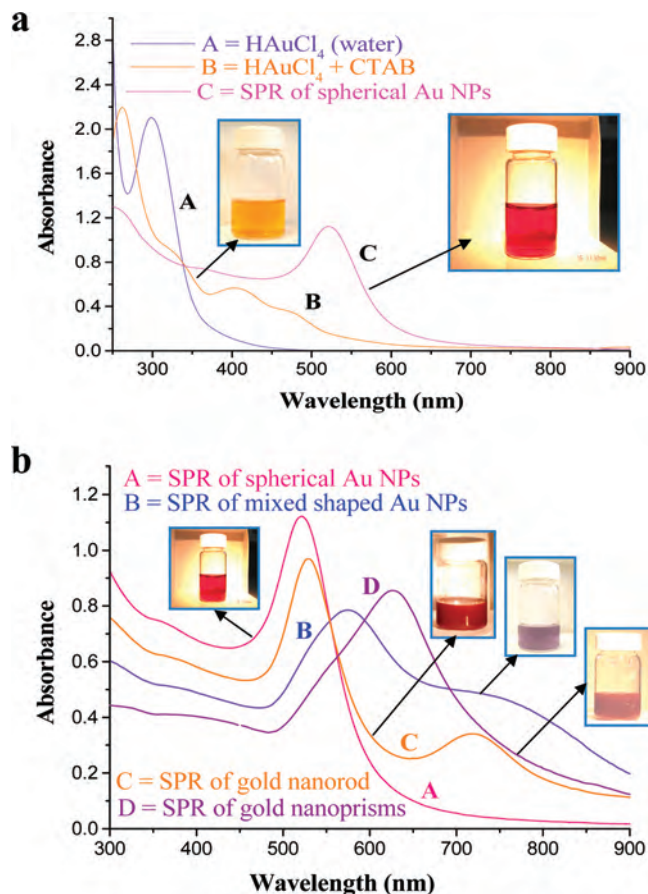


Figure 1. (a) UV–visible absorption spectra at various stages of gold NPs synthesis. A, absorption spectra of gold chloride (HAuCl_4) solution in water; B, absorption spectra of HAuCl_4 in CTAB micellar solution; C, Surface Plasmon Resonance (SPR) band for spherical gold NPs. Inset shows the image of orange color CTAB-Au(III) complex and pink color spherical gold NPs solution. (b) UV–visible absorption spectra of four different gold NPs solution having different shapes. A, SPR band of spherical gold NPs; B, SPR band of mixed shaped gold NPs; C, SPR band of gold nanorods; and D, SPR of gold nanoprisms. All the spectra were recorded after 90 s of MW heating. Inset shows four different color gold NPs solution.

equipped with 1 cm quartz cuvette holder for liquid samples. A high resolution-transmission electron microscope (HR-TEM) (ZEOL ZEM 2010) was used at an accelerating voltage of 200 kV. The energy dispersive X-ray spectrum (EDS) was recorded with the Oxford Instruments INCA energy system connected with the TEM. The X-ray diffraction (XRD) analysis was done with a scanning rate 0.020 s^{-1} in the 2θ range $20\text{--}80^\circ$ using a Rigaku $\text{D}_{\text{max}} \gamma_{\text{A}}$ X-ray diffractometer with $\text{Cu K}\alpha$ radiation ($\lambda = 0.154178$). Atomic force microscopy (AFM) images were generated with a multimode atomic force microscope (AFM, Pacific Nanotechnology Inc.). Field emission scanning electron microscopy (FE-SEM) images were obtained using a Zeiss SEM ultra 60. A domestic microwave (MW) oven (Gold star company, EM-Z200S, 1000 W, 60 Hz) was used for MW irradiation for the entire synthesis.

Preparation of Multiple Shapes Gold Nanoparticles. Spherical gold NPs were prepared by mixing 4 mL of CTAB (10^{-2} M) solution with 200 μL of (10^{-2} M) aqueous Au (III) solution. After that 2 mL of aqueous 2,7-DHN solution was added to the reaction mixture such that the final concentration became 3.17×10^{-3} M. Finally 100 μL of (1 M) NaOH was added, and the mixture was stirred for 30 s and then irradiated by MW for 90 s with an intermittent pause after every 10 s to cool the reaction vessel. For the synthesis of anisotropic gold NPs we vary the concentration of 2,7-DHN and NaOH keeping the other concentration fixed. The

- (18) Harpeness, R.; Gedanken, A. *Langmuir* **2004**, *20*, 3431.
 (19) Pastoriza-Santos, I.; Liz-Marzán, L. *Langmuir* **2002**, *18*, 2888.
 (20) Chen, W.; Zhao, J.; Lee, J. Y.; Liu, Z. *Mater. Chem. Phys.* **2005**, *91*, 124.
 (21) Panda, A. B.; Glaspell, G. P.; El-Shall, M. S. *J. Am. Chem. Soc.* **2006**, *128*, 2790.
 (22) Jin, R.; Cao, Y.; Mirkin, C. A.; Kelly, K. L.; Schatz, G. C.; Zheng, J. G. *Science* **2001**, *294*, 1901.
 (23) Sankar, S. S.; Rai, A.; Ankamwar, B.; Singh, A.; Ahmed, A.; Sastry, M. *Nat. Mater.* **2004**, *3*, 482.
 (24) Ha, T. H.; Koo, H.-J.; Chung, B. H. *J. Phys. Chem. C* **2007**, *111*, 1123.

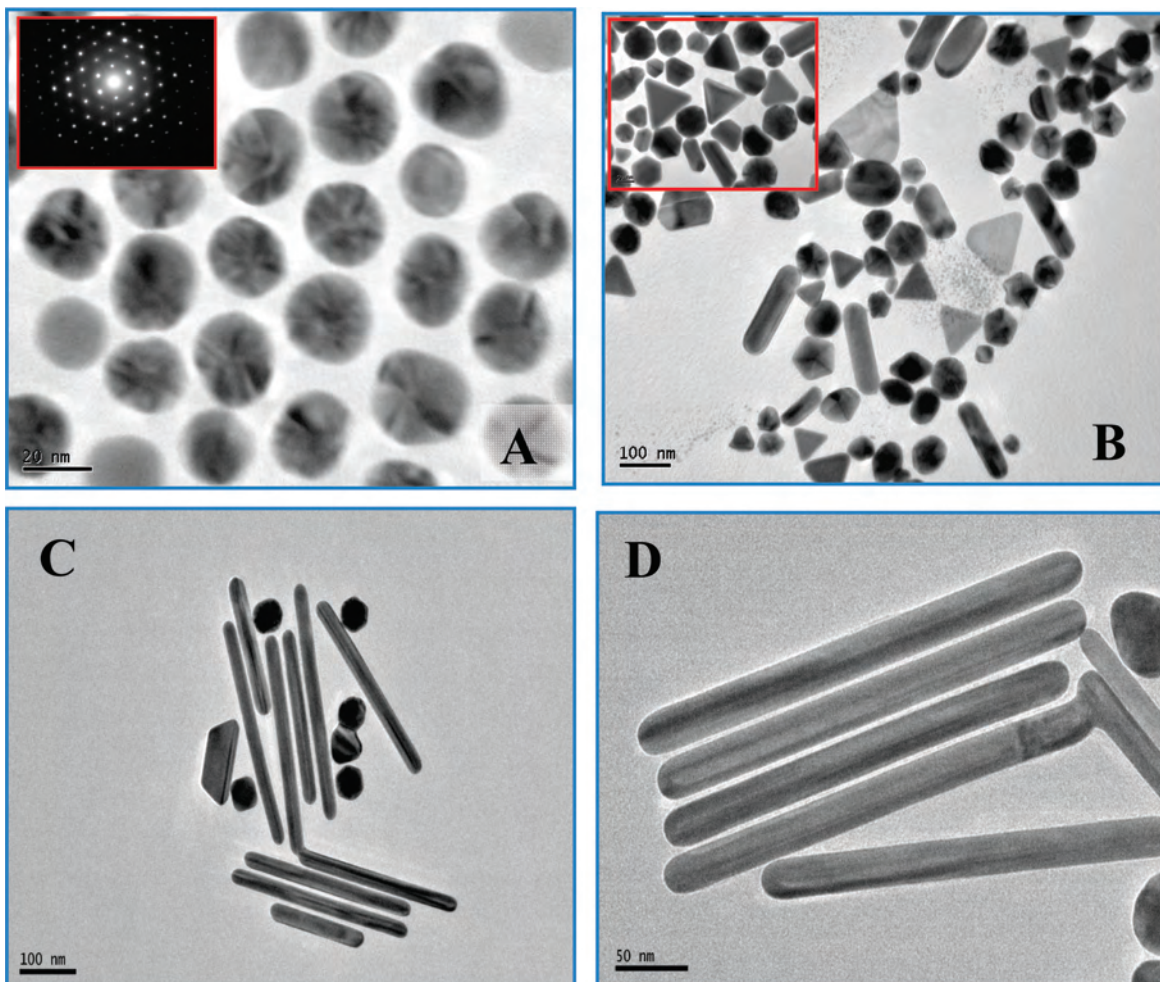


Figure 2. TEM image of different shaped gold NPs synthesized after 90 s of MW exposure. (A) Image of spherical gold NPs; (B) low magnified images of mixed (mixture of different shapes) shaped gold NPs; C and D show the images of gold nanorods at different magnification. The inset of A and B shows the corresponding electron diffraction of the particles and a higher magnified image.

final concentrations of 2,7-DHN and NaOH were 1.05×10^{-3} M and 1.05×10^{-2} M, respectively. For rod shaped particles the final concentrations of CTAB, Au(III), 2,7-DHN, and NaOH were 7.54×10^{-3} M, 4.71×10^{-4} M, 1.88×10^{-3} M, and 9.43×10^{-3} M, respectively. For nanoprism synthesis, a mixer was prepared with 4 mL of (0.1 M) CTAB, 320 μ L of (10^{-2} M) Au (III) solution, 280 μ L of (10^{-2} M) 2,7-DHN, and 10 μ L of (1 M) NaOH. The solution was stirred for 30 s and irradiated by MW for 90 s. For all the above cases, the Au particles' formation started just after 10–20 s of MW irradiation as observed from the color change of the solution mixture and from the UV–visible spectrum. The resulting solution was centrifuged at 3000 rpm for 10 min for the removal of excess surfactants. The precipitate was redispersed in DI water and centrifuged again at 2000 rpm for 5 min. This process was repeated twice. Finally, the precipitate Au NPs was collected and redispersed in water for characterization. The solution became deep pink (for spherical), bluish pink (for mixed shapes), bluish purple (for rod shapes), and pinkish red (nanoprisms) after completion of the reaction. The color remained stable for at least 3 months in dark under ambient environment without change in optical properties.

Preparation of Samples for HR-TEM, FE-SEM, and AFM Analysis. The samples for TEM analysis were prepared by placing a drop of fresh NPs solution on a carbon-coated copper grid followed by slow evaporation of the solvent at ambient condition. The FE-SEM and AFM studies were performed on a Si-chip with

a native oxide layer. The chip was rinsed thoroughly with ethanol and piranha (30% H_2O_2 and 70% H_2SO_4) followed by final cleaning with ethanol and acetone. The chip was then air-dried and dipped in 0.1 wt % solution of PSS overnight followed by a vigorous wash to remove excess PSS leaving a monolayer. The sample was then blow-air-dried and placed on a gold NPs solution for 30 min to deposit gold nanoprisms.

Results and Discussion

The Au NPs were synthesized by the reduction of Au(III) ions in the presence of alkaline 2,7-DHN using CTAB as a stabilizing agent in a 1000 W MW oven. Figure 1a shows the UV–visible spectrum of the solution mixture at various stages of the process. The light yellowish color of the aqueous HAuCl_4 solution exhibits an intense absorption band at 292 nm (curve A, Figure 1a) because of a metal–ligand charge transfer (MLCT) band from the AuCl_4^- complex.²⁵ The light yellowish color of the aqueous HAuCl_4 solution changes to deep orange having three characteristic absorption peaks at 262 nm, 326 nm, and 402 nm with the addition of CTAB with HAuCl_4 (curve B, Figure 1a). This orange color is due to 1:1 complex formation of CTAB with aqueous

(25) Roy Meson, W.; Gray, H. B. *Inorg. Chem.* **1968**, *7*, 55.

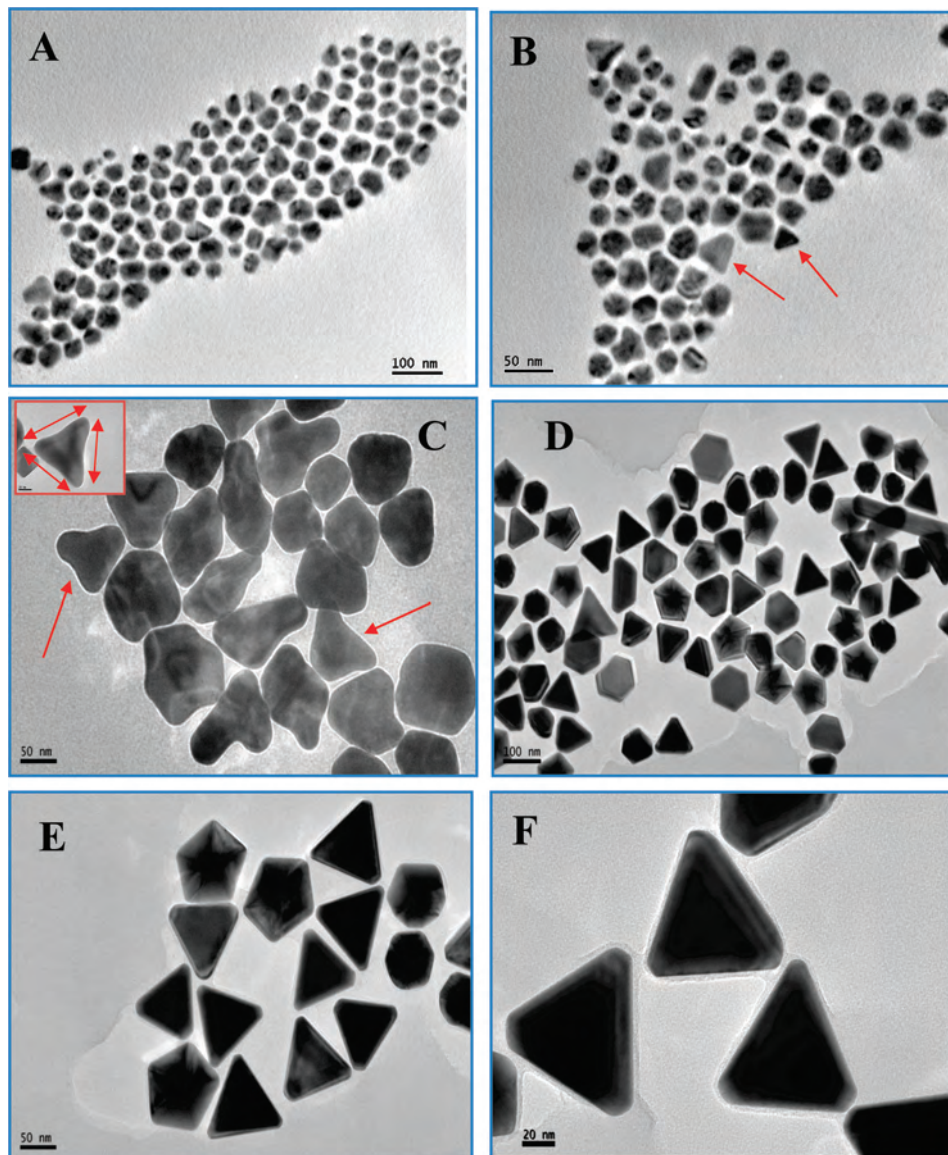


Figure 3. TEM images for the synthesis of gold nanoprisms under different MW exposure times. A, B, and C are the TEM images after 30 s, 45 s, and 60 s MW exposure, respectively. D and E are the low and high magnified images after 90 s MW exposure. F is the image after 90 s MW exposure after 3 months aging in air. The inset of C shows a corresponding higher magnified image of single particles.

HAuCl₄ solution. The three peaks are assigned for the vibrational frequencies of [AuBr₂]⁻ (at 262 nm), Au(III) in CTAB (at 326 nm), and the ion-pair formation of [CTA]⁺[AuBr₄]⁻ (at 402 nm), where [CTA]⁺ = cetyl trimethyl ammonium ion.^{26,27} Now, addition of alkaline 2,7-DHN with the orange complex and subsequent MW heating, the color changed to pink with the appearance of a new peak at 520 nm because of surface plasmon resonance (SPR) of spherical gold NPs (curve C, Figure 1a).^{28–31} The formation of a pink color started after 30 s of MW heating as observed from the UV–visible spectrum, increased gradually with the increase in microwave exposure, and saturated after 90 s

indicating the completion of the reaction. The inset of Figure 1a shows the image of brown complex and pink spherical Au NPs solution. Addition of NaOH and 2,7-DHN in different concentration with the reaction mixture (containing HAuCl₄ and CTAB) and subsequent microwave exposure produced anisotropic Au NPs. In this case, the solution color changed from pink to purple, bluish purple to pinkish red depending upon the concentration of 2,7-DHN and NaOH. Figure 1b shows the UV–visible spectrum of the different gold NPs solution. In Figure 1b, curves A, B, C, and D denote the SPR band for spherical, polygonal (mixed shaped), rods, and triangular gold NPs respectively. The spectrum B containing the mixture of anisotropic particles shows two intense absorption peaks, one at ~ 576 nm and another broad peak >700 nm. The spectrum C, containing the nanorods, shows two peaks, one at 530 nm (due to transverse SPR) and another peak at 720 nm (due to longitudinal SPR). The spectrum D, containing the nanoprisms, shows a broad peak,

- (26) Chen, S.; Carroll, D. L. *J. Phys. Chem. B* **2004**, *108*, 5500.
 (27) Aguirre, C. M.; Kaspur, T. R.; Radloff, C.; Halas, N. J. *Nano. Lett.* **2003**, *3*, 1707.
 (28) Jana, N. R.; Gearheart, L.; Murphy, C. J. *Langmuir* **2001**, *17*, 6782.
 (29) Jana, N. R.; Gearheart, L.; Murphy, C. J. *Adv. Mater.* **2001**, *13*, 1389.
 (30) Zhu, J. J.; Liu, S. W.; Palchik, O.; Koltypin, T.; Gedanken, A. *Langmuir* **2000**, *16*, 6396.
 (31) Kundu, S.; Maheshwari, V.; Saraf, R. F. *Langmuir* **2008**, *24*, 551.

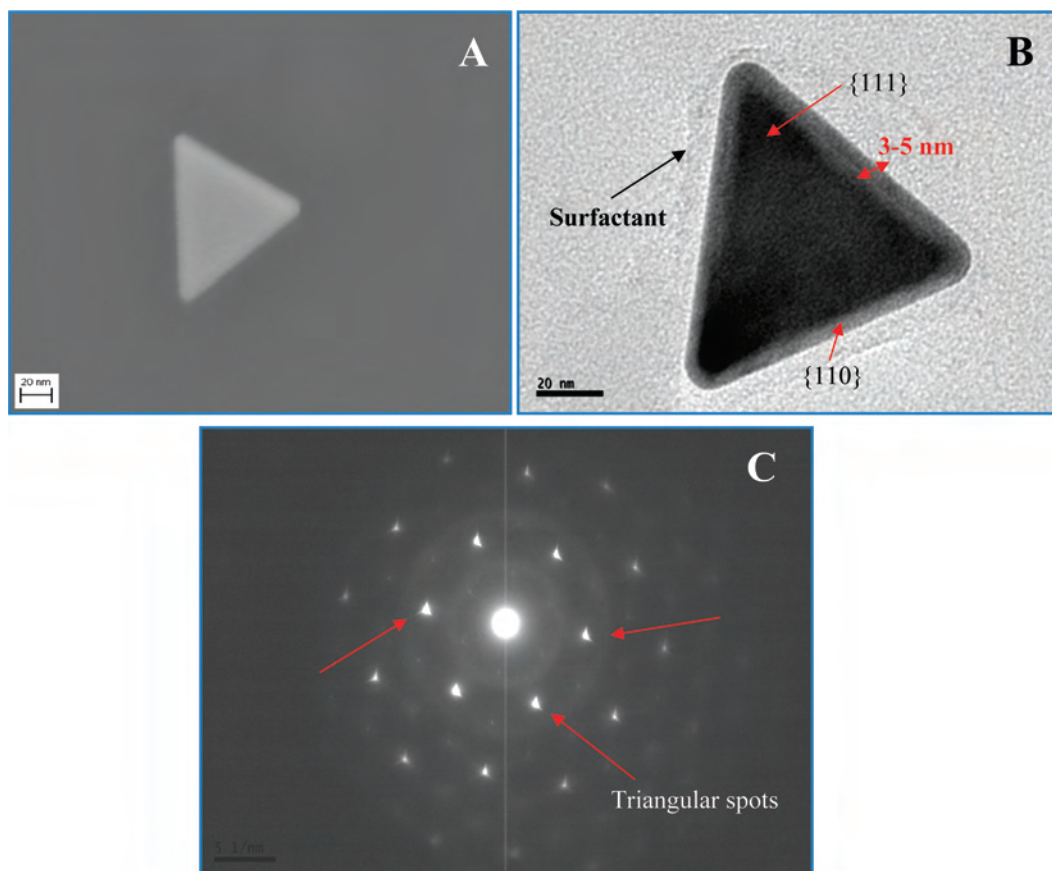


Figure 4. FESEM and TEM image of single gold nanoprisms synthesized after 90 s of MW exposure. (A) FESEM images of single gold nanoprisms and (B) TEM image of single gold nanoprisms. C is the electron diffraction pattern of single prisms obtained by TEM and shows that the particles are single crystal.

at ~ 630 nm. Similar types of absorption spectra for nanorods^{13,28,29} and nanoprisms^{23,24,32} were also observed by other researchers. The inset of the Figure 1b shows the different-colored Au NPs solutions corresponding to curves A, B, C, and D for different shapes, respectively. The significant difference in the optical properties of the nanorods and nanoprisms, as compared to the spherical particles, is responsible for the broad peak >600 nm in the longer wavelength side resulting from the anisotropic structure (rod, wires, cubes, etc.).³³ It is noticeable that the final product has high yield (~ 80 – 85% rods and $\sim 95\%$ prisms), significantly higher than the reported ones (~ 45 – 50%).^{13,23}

Figure 2 shows the transmission electron microscopy (TEM) images of various CTAB capped Au NPs prepared with the above method. Figure 2A shows the TEM image of the low magnified spherical Au nanoparticles corresponding to curve C in Figure 1a. The average size of the particles is 25 ± 2 nm. Figure 2B shows the mixture of different shaped particles containing spheres ($\sim 16\%$), triangles ($\sim 22\%$), rods ($\sim 10\%$), hexagonal shapes ($\sim 28\%$), and a few other shaped particles. Figure 2C and 2D has the images of the nanorods at different magnification. The average length of the rods is around ~ 300 nm and the width ~ 25 nm corresponding to an aspect ratio of ~ 12 . The inset of Figure

2A shows the corresponding selected area electron diffraction (SAED) pattern of the gold nano spheres indicating that the particles are a single crystal. We studied the growth mechanism of the particles' formation with different MW exposure time taking triangular particles as an example. Figure 3 shows the TEM images of the Au nanoprisms at various stages of the microwave heating. Figure 3A,B shows the TEM image of the formation of Au nanoprisms after 30 and 45 s of MW heating, respectively. The particles are $\sim 40 \pm 10$ nm in diameter having no defined shape and started to grow into the triangular shape. Figure 3C shows the low magnified image after 60 s of MW heating with particles perfectly grown into triangular shapes. This is clearly seen in the high magnification image of a single particle (inset of Figure 3C). Figure 3D and 3E shows the different magnified images of nanoprisms after 90 s of MW heating. The image contains $>95\%$ of prisms with a few other shaped particles having average particle size $\sim 65 \pm 10$ nm. Inside the particles, the contrast changes might be due to the internal stress of the on-growing crystal layers. The thickness of the prisms is 3.5–4 nm calculated from the AFM height profile. Figure 3F shows the TEM image of the gold nanoprisms after aging for 3 months in air. The particles' size and shape were almost unchanged (similar to Figure 3D and 3E) indicating the high stability of the nanoprism solution.

Figure 4 shows TEM and field emission scanning electron microscopy (FESEM) images of a single nanoprism. Figure

(32) Xue, C.; Millstone, J. E.; Li, S.; Mirkin, C. A. *Angew. Chem.* **2007**, *119*, 8588.

(33) Chen, S.; Wang, Z. L.; Ballato, J.; Foulger, S. H.; Carroll, D. E. *J. Am. Chem. Soc.* **2003**, *125*, 16186.

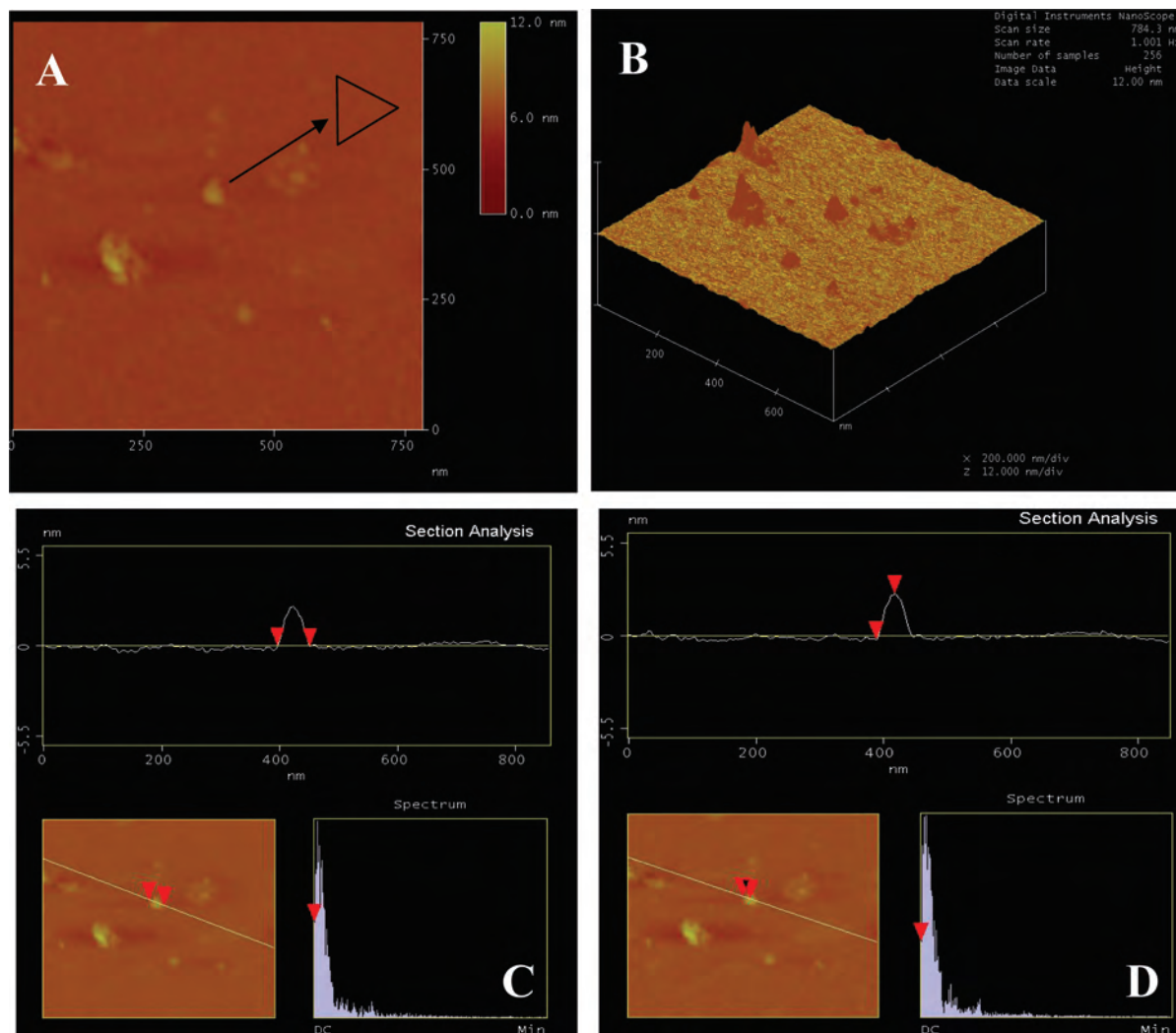


Figure 5. AFM images of gold nanoprisms. Topographic (A) and 3-D (B) image of the triangular nanoparticle. The line profile shows that the width (C) of a triangular nanoparticle is about 55–60 nm and the height (D) of a triangular nanoparticle is 3.5–4 nm.

4A corresponds to the FESEM image, and 4B corresponds to the TEM image of a single nanoprism. The side length of the prism is the same for both techniques. Figure 4C shows the selected area electron diffraction (SAED) pattern in the corresponding area obtained from TEM. The SAED proves that the particles are single crystalline in nature. The diffraction spots exhibit the triangular shape. This type of well defined shape effects as a result of nanoprisms has not been reported before.

The AFM images of gold nanoprisms are shown in Figures 5A and 5B. Figure 5A is the topographic image while 5B is the 3-D mode. The line profile shows the width of the particles, $\sim 55\text{--}60$ nm (Figure 5C), and the height, $\sim 3.5\text{--}4$ nm (Figure 5D). The AFM results perfectly match with the results obtained from TEM and SEM studies.

The effects of NaOH concentration on NP synthesis was examined in detail. The reducing capacity of any hydroxyl compounds strongly depends on the pH of the reaction medium. In our experiments, while in the presence of microwave heating and the absence of NaOH (other parameters fixed), there were no gold nanoparticles formed. On the contrary, the gold nanoparticles were formed with addition of NaOH. With the increase in pH of the reaction

mixture (pH $\sim 7.5\text{--}8.5$), the SPR band for gold nanoparticles red-shifted, indicating the formation of anisotropic Au nanoparticles. The facilitated formation of nanorods and nanoprisms at higher pH values should be understood on the grounds that the reduction power of 2,7-DHN can be strengthened because of the elimination of protons produced by reduction. With further increased pH, a blue solution was seen with some aggregated particles. In this case there were no clearly defined shaped particles, as shown in Figure 6. This is probably due to the hydroxyl compound of gold or Au_2O in the highly alkaline condition. A similar observation was reported by Chen et al.³³ It was reported earlier that the hydroxyl ion concentration directs the growth of metal nanoparticles in different shapes.^{34,35} The feasible formation of a definite shape with an addition of small amount of NaOH has also been observed in a previous report by Mirkin et al.³⁶ In our experiments, a proper OH^- concentration assists the growth of the particles in selective crystallographic

(34) Panigrahi, S.; Kundu, S.; Ghosh, S. K.; Nath, S.; Praharaj, S.; Basu, S.; Pal, T. *Polyhedron* **2006**, *25*, 1263.

(35) Jana, N. R.; Gearheart, L.; Murphy, C. J. *J. Phys. Chem. B* **2001**, *105*, 4065.

(36) Millstone, J. E.; Park, S.; Shuford, K. L.; Qin, L.; Schatz, G. C.; Mirkin, C. A. *J. Am. Chem. Soc.* **2005**, *127*, 5312.

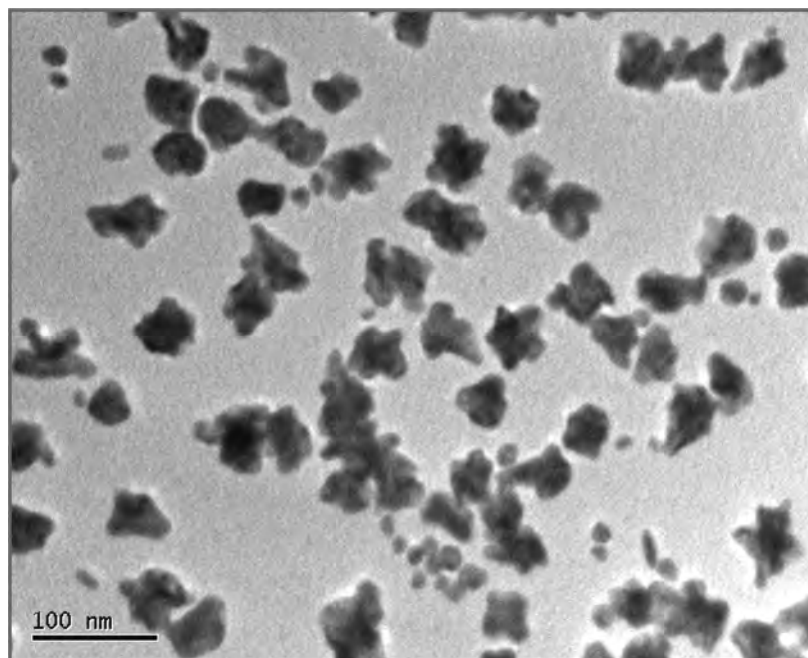
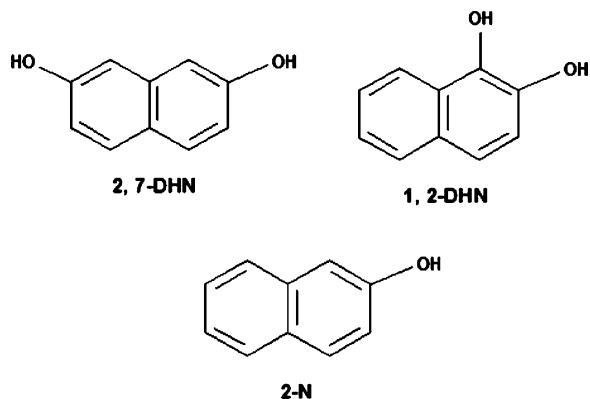


Figure 6. TEM image of gold NPs with higher concentration of NaOH (pH \sim 10).

Table 1. Concentrations of the Reaction Variables, Average Size, and Shape of Gold NPs after 90 s MW Exposure

| conc. of HAuCl ₄ solution (M) | conc. of CTAB (M) | conc. of 2,7-DHN (M) | conc. of NaOH (M) | MW time (s) | average size (final, nm), (λ_{\max}) | shape distribution |
|--|-----------------------|-----------------------|-----------------------|-------------|--|--|
| 3.17×10^{-4} | 6.34×10^{-3} | 3.17×10^{-3} | 1.15×10^{-2} | 90 | 25 ± 2 (520) | 100% spherical |
| 4.21×10^{-4} | 8.42×10^{-3} | 1.05×10^{-3} | 1.05×10^{-2} | 90 | 50–120 (576 and >700) | spheres (\sim 16%), triangles (\sim 22%), rods (\sim 10%), hexagonal shapes (\sim 28%), and few other shaped particles |
| 4.71×10^{-4} | 7.54×10^{-3} | 1.88×10^{-3} | 9.43×10^{-3} | 90 | aspect ratios \sim 12 (530 and 720) | \sim 75–80% rods; and rest, spheres |
| 6.94×10^{-4} | 8.68×10^{-2} | 6.07×10^{-4} | 1.73×10^{-4} | 90 | 65 ± 10 (630) | 95% prisms; and rest, hexagonal and other shapes |

Scheme 1. Chemical Structure of 2,7-Dihydroxy Naphthalene (2,7-DHN), 1,2-Dihydroxy Naphthalene (1,2-DHN), and 2-Naphthol (2-N)



directions leading to the shape control. For the synthesis of nanorods and nanoprisms we fixed the NaOH concentration to 9.43×10^{-3} M and 1.73×10^{-4} M respectively (Table 1).

We have examined the CTAB concentration from 10^{-1} M to 10^{-4} M. In the absence of CTAB, the micron sized gold particles are formed as observed from TEM (not shown here) but precipitated immediately because of the absence of any stabilizer in the aqueous solution. The different concentrations of CTAB used for different shapes were shown in Table 1. It was reported earlier that high concentration of CTAB (0.1 M) enhanced the formation of gold

nanorods and other anisotropic particles because of the formation of an elongated micellar template.^{28,35,37} Similarly, in our case, the nanoprisms only formed at high concentration of CTAB (9.6×10^{-2} M). In our previous studies, it was reported that the gold nanocubes¹⁵ could be formed in relatively low concentration of CTAB (6.3×10^{-3} M) in the presence of UV light irradiation.

In our experiments an alkaline solution of 2,7-DHN was used as a new reducing agent for the formation of gold NPs. In the absence of 2,7-DHN while keeping other reaction parameters the same, a turbid brown solution was formed because of the formation of a $[\text{CTA}]^+[\text{AuBr}_4]^-$ or $[\text{AuBr}_4]^-/[\text{AuBr}_2]^-$ complex. The variation of the 2,7-DHN concentration affected the formation of NPs as a result of the formation of spherical or other shaped particles. The detailed reaction conditions are listed in Table 1. We have studied reactions with other hydroxyl compounds that have similarity with 2,7-DHN including 1,2-dihydroxynaphthalene (1,2-DHN), 2-naphthol (2-N), and so forth (Scheme 1). The preliminary study indicates that the formation of gold NPs and the detailed results will be reported elsewhere.

Figure 7A and 7B presents the results obtained from EDS and XRD pattern analysis, respectively. All the diffraction peaks can be indexed to the characteristic peaks of gold NPs. The Bragg reflection obtained from the gold nanoprisms

(37) Tornbolm, M.; Henriksson, U. *J. Phys. Chem. B* **1997**, *101*, 6028.

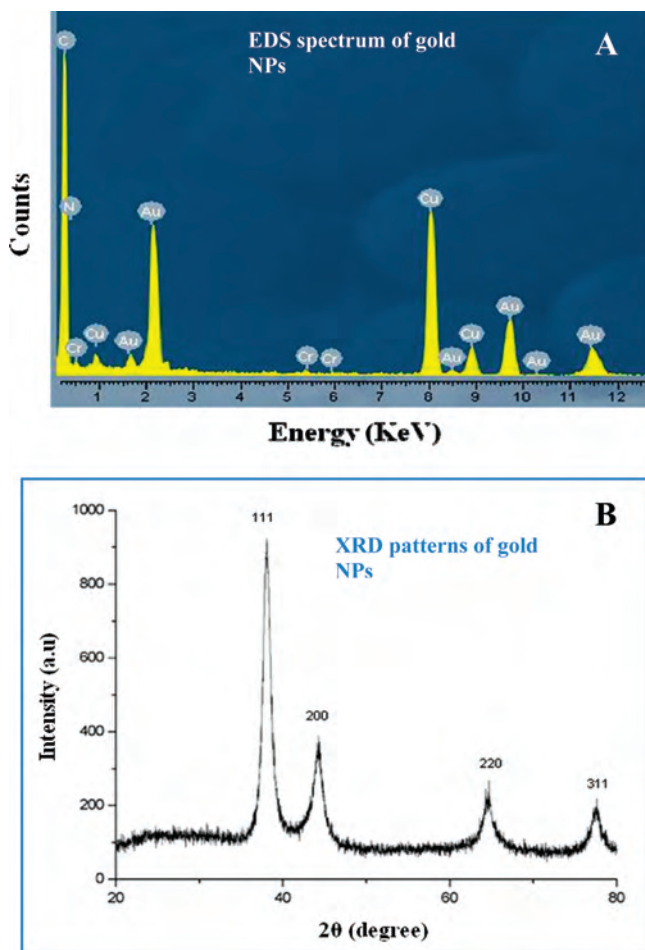


Figure 7. (A) EDS and (B) powder XRD pattern of the gold NPs.

clearly corresponds to the fcc crystalline structure of gold.³⁸ The peaks are assigned to the diffraction from the (111), (200), (220), and (311) planes of fcc gold, respectively. An overwhelmingly strong diffraction peak located at 44.19° is ascribed to the {111} facets of face centered cubic metal structure. The normal orientation of the observed flat nanoprisms was assigned as the {111} direction as hexagonal patterns on the spectrum are lying flat on the planner surface.

The formation of anisotropic gold NPs initiated by the reduction of Au(III) ions by the phenolic compound, 2,7-DHN in alkaline medium, in presence of MW heating. The use of these phenolic compounds for NPs synthesis is not expected. It was reported that most phenolic compounds such as benzophenone,³⁹ dendrimer,⁴⁰ polyvinyl alcohol,⁴¹ ascorbic acid,⁴² TX-100,⁴³ and so forth underwent photolytic cleavage to a phenoxy radical in the presence of UV light or at high temperature. In the present work, it was assumed that the radicals or the solvated electrons formed during the MW heating of a solution mixture containing 2,7-DHN

enabled the reduction of Au(III) to Au(0). When the nucleation of Au(0) starts, the growth takes place in multiple steps and produces different anisotropic particles. The reduction of Au(III) to Au(0) leads to the formation of small spherical nuclei. The nuclei subsequently form Au atoms and assemble them together into a crystalline particle. The surfactant CTAB molecule is attached to the surface of these crystals and thus slows down the growth rate of the crystal facets. When the surfactant concentration is less ($\leq 10^{-2}$ M), the interaction of the cationic parts with the specific surface is weak. As a result, the growth of particles takes place in all directions leading to the formation of spherical particles. With a high surfactant concentration (10^{-1} M or higher), the cationic CTAB in aqueous solution formed polygonal micellar shapes (rod like and others) as reported by Murphy et al.^{28,35} The shape of the rod-like micelle promotes the formation of rod like nanomaterials.¹³ Here, in our study, we believe that at that particular concentration CTAB forms the rod like “micellar template” and interacts strongly with the growing crystal facets of gold and generates gold nanorods. But for the nanoprism synthesis in other CTAB concentrations, some trimeric clusters might be formed in the solution having similarity with the formation of triangular nanoplates of silver done by Xia’s group.⁴⁴ Now during the nucleation stage, the trimeric clusters generate triangular nuclei. With the increasing MW time, the Au atoms added more on the growing triangular nuclei, and they converted to either the triangular shape or the truncated one depending upon the ratio of {111} to {100} facets over the other side facets. In our study we observed mostly triangular nanoprisms as confirmed from TEM images in Figure 3D and 3F. The CTAB tends to attach to the lowest energy {111} facet and suppress the growth rate of this facet. The cationic headgroup of CTAB interacts strongly with the {111} facets of Au particles. The {111} facets of gold are more reactive than the other facets like {110} or {100} in the presence of bromide ion leading to the formation of nanoprisms. As a result this stabilizes the formation of a bilayer structure due to the van der Waals interaction between hydrophobic groups. According to the TEM images in Figure 3, it is clear that after a short time of MW heating small spherical particles were formed. With the increased MW heating time, these small particles grew into bigger particles in certain crystallographic directions resulting in nanoprisms. The surfactant CTAB was adsorbed on the particular faces of the gold crystal and directed the 3D growth. Formation of well-defined-shaped particles depends on the faceting tendency of the stabilizing agent and on the growth kinetics (rate of Au(0) supply to the crystallographic planes).⁴⁵ The long alkyl chain of the CTAB molecule always anchors to the Au(0) surface.⁴⁶ In our research, NPs were found well separated from each other. This is due to the CTAB adsorption on the particle surface as a protective shell from aggregation.

In summary, we presented a new chemical route for the synthesis of shape-controlled gold NPs in large scale. The process was successful for making multiple shapes (spheres,

(38) Guinier, A. *X-Ray Diffraction*; W. H. Freeman: San Francisco, CA, 1963.

(39) Sato, T.; Maeda, N.; Ohkoshi, H.; Yonezawa, Y. *Bull. Chem. Soc. Jpn.* **1994**, *67*, 3165.

(40) Esumi, K.; Suzuki, A.; Aihara, N.; Usui, K.; Torigoe, K. *Langmuir* **1998**, *14*, 3157.

(41) Henglein, A. *Langmuir* **1999**, *15*, 6738.

(42) Pal, A.; Pal, T. *J. Raman. Spectrosc.* **1999**, *30*, 199.

(43) Pal, A. *Talanta* **1998**, *46*, 583.

(44) Xiong, Y.; Washio, I.; Chen, J.; Sadilek, M.; Xia, Y. *Angew. Chem.* **2007**, *119*, 5005.

mixed shapes, rods, and prisms) in a short time (60–90 s) under MW heating in the presence of CTAB and alkaline 2,7-DHN. The synthesized particles were found to be stable for at least 3 months. With the variation of surfactant to metal ion molar ratio, the particles size and shape were successfully modified. The approach developed here would lead to the formation of other metallic (like Ag, Pd, Pt, etc.) and semiconductor (CdS, CdSe, CdTe, etc.) particles with well-defined shapes. There are promising applications for this in many areas such as catalysis, clinical and diagnostic medicine, and nanoelectronics, among others.

(45) Petroski, J. M.; Wang, Z. L.; Green, T. C.; El-Sayed, M. A. *J. Phys. Chem. B* **1998**, *102*, 3316.

Acknowledgment. This research was in part sponsored by the NSF-0506082; the Department of Mechanical Engineering, Texas A & M University; and the Texas Engineering Experiments Station. Supports for TEM and EDS by Dr. Zhiping Luo at the Microscopy Imaging Center (MIC), Texas A & M University and for HR-SEM by Dr. Dwight Romanovicz at the Biological Science Department, University of Texas, Austin were greatly appreciated.

IC8004135

(46) Praharaj, S.; Ghosh, S. K.; Nath, S.; Kundu, S.; Panigrahi, S.; Basu, S.; Pal, T. *J. Phys. Chem. B* **2005**, *109*, 13166.